*Optica Applicata, Vol. LIV, No. 1, 2024*
DOI: 10.37190/oa240105

# Radio-over-fibre for generation and transmission 32-tupling frequency optical millimeter wave with polarization modulators

Xinqiao Chen[1,*], Siyuan Dai[1], Xiaorui Liu[2], Xu Chen[1], Zhihan Li[1]

[1]School of Information and Communication Engineering, Communication University of China, Beijing 100024, China

[2]School of Electronic Engineering, Beijing University of Posts and Telecommunications, China

[*]Corresponding author: chenxinqiao9999@163.com

A novel structure to generate 32-tupling frequency millimeter-wave (MMW) signal using polarization modulators (PolM) is proposed. The ±16th order sidebands are generated by the 16th order sidebands generator which is mainly constructed by six PolMs and beat in a photodetector for generating the 32-tupling frequency MMW. The optical sideband suppression ratio (OSSR) of the generated ±16th order sidebands are 29.89 and 29.7 dB from theoretical analysis and simulation. The radio frequency (RF) spurious suppression ratio (RFSSR) of the obtained 32-tupling frequency MMW are 23.88 and 23.32 dB from theoretical analysis and simulation. A radio over fiber (ROF) system to transmit the generated 32-tupling frequency MMW is built. In the center station, the +16th order sideband from the ±16th order sideband generator is filtered out by a filter, after the downlink data is modulated on it. It is recombined with –16th order sideband and transmitted to the based station over fiber. In the based station, a part of –16th order sideband is reflected by a fiber Bragg grating (FBG), and the uplink data is modulated on it and transmitted to the center station over fiber. The signal emerging from the FBG is injected into the photodetector and the 32-tupling frequency MMW with downlink data is generated. The simulation results show that for the transmission fiber length 30 km, the bit-error-rate (BER) is less than $10^{-9}$, the power cost of the uplink and downlink is less than 0.44 and 0.5 dB, respectively.

Keywords: radio-over-fiber (ROF), millimeter-wave (MMW), polarization modulator (PolM), Mach –Zehnder interferometer (MZI), optical sideband suppression ratio (OSSR), radio frequency spurious suppression ratio (RFSSR).

## 1. Introduction

The radio over fiber (ROF) technology combines the advantages of optic fiber communication and wireless communication and it is one of the key technologies for future ultra-broadband wireless access [1,2]. In recent years, with the development of wireless communication technology, the carrier frequency has been moving into the band of millimeter wave (MMW). The generation of MMW in electric domain is lim-

ited by the electronic bottleneck of electronic devices, which makes it difficult to generate MMW with frequencies above 100 GHz. The generation of MMW in the optical domain can overcome this limit and it is the key technology in the ROF [3-5]. At present, the main proposed methods to generate optical MMW include direct modulation [6], optical heterodyne [7], four-wave mixing [8] and stimulated Brillouin scattering [9], external modulation [10-18], *etc*. Among the above methods, the external modulator method is the main method to generate optical MMW. Among the external modulator methods, the methods based on Mach–Zehnder modulator (MZM) have many advantages, such as low complexity, low cost, *etc*. However, this method suffers from the bias drift problem and requires sophisticated bias control circuits. The methods to generate optical MMW with polarization modulator (PolM) do not need direct current (DC) bias, and it has become a research hotspot in recent years at home and abroad.

The frequency of the generated MMW based on the PolM methods is $2nf_{RF}$, where $f_{RF}$ is the frequency of the radio frequency (RF) driving signal which is loaded on the PolM, $n$ is the desired order of optical sidebands generated by the PolMs, $2n$ is frequency multiplication factor (FMF). Since the increase of $f_{RF}$ is limited by the electronics, the main method to increase the frequency of MMW is to increase the FMF. In [10], LIU *et al*. proposed a scheme to generate quadruple frequency MMW with a PolM. In [11], a method to generate 6-tupling frequency MMW using a PolM and a fixed-wavelength trap filter was proposed. In [12], YANG *et al*. proposed a structure to generate 8-tupling frequency MMW with two cascaded PolMs. In [13], ABOUELEZ proposed a method to generate 12-tupling frequency MMW generation with two cascaded dual parallel polarization modulators (DP-PolM). In [14,15], BASKARAN *et al*. proposed a scheme to generate 16-tupling frequency MMW using four PolMs connected in parallel, and in the same year, they proposed a structure to generate 16-tupling frequency MMW using four PolMs. In [16], CHAUDHURI *et al*. proposed a scheme to generate 24-tupling frequency MMW and obtained 60 GHz MMW with 2.5 GHz RF driving signal.

In the above methods to generate MMW with PolM, the largest FMF is only 24. In order to increase the FMF, our research group proposed two filterless methods to generate 32-tupling MMW based on DP-PolMs [17,18]. In order to compare the performance of the main methods proposed so far to generate MMW based on PolM, we tabulate the main parameter of those methods in Table 1.

In [17], it needs eight PolMs, because the system is complicated and costly. In [18], in order to suppress the optical carrier in the output signal, the polarization multiplexing method is adopted. This method requires to control the polarization angle of polarizer accurately and is susceptible to the polarization state of optical signals.

In the methods to generate 32-tupling frequency MMW, in order to reduce the system cost [17] and eliminate the effect of polarization state on the system [18], we propose a new method to generate 32-tupling MMW with six PolMs. The carrier in the output is suppressed by adjustable optical attenuator (OATT) and π optical phase shifter (OPS).

T a b l e 1. The main methods to generate MMW based on PolM.

| References | Year | Architecture | Method | FMF | OSSR [dB] | RFSSR [dB] |
|---|---|---|---|---|---|---|
| | | | | | Theory/Simulation | Theory/Simulation |
| LIU *et al*. [10] | 2013 | Single PolM+Sagnac | Experiment | 4 | /42 | /17.8 |
| LI and YAO [11] | 2010 | Single PolM+Notch filter | Experiment | 6 | /21 | /15 |
| YANG *et al*. [12] | 2015 | Two cascaded PolMs | Experiment | 8 | /37 | /37.5 |
| ABOUELEZ [13] | 2020 | 2 cascaded DP-PolMs | Simulation | 12 | /25.1 | /19.1 |
| GAYATHRI and BASKARAN [14] | 2019 | 4 Parallel PolMs | Simulation | 16 | /62 | /36 |
| BASKARAN *et al*. [15] | 2019 | 4 PolMs parallel serial mixing | Simulation | 16 | 63.4/63 | 51.8/51 |
| CHAUDHURI *et al*. [16] | 2020 | Cascade Dual Parallel PolMs | Simulation | 24 | 37.87/34.4 | 25.84/25.8 |
| CHEN *et al*. [17] | 2021 | 8 Parallel PolMs | Simulation | 32 | 55.7/53.38 | 43.66/42 |
| CHEN *et al*. [18] | 2022 | Cascade Dual Parallel PolMs | Simulation | 32 | 53.7/52 | 47.7/47 |

## 2. System design

Figure 1 is the schematic diagram to generate 32-tupling frequency MMW with six PolMs. The main devices in the structure are a CW laser, a polarization controller (PC), a two optical phase shifters (OPS1, OPS2), two optical adjustable attenuators (OATT1, OATT2), two polarizers (Pol1, Pol2), a RF signal generator, four electrical phase shifters (EPS1...EPS4), two optical amplifiers (OA1, OA2), a photodetector (PD), twelve 3 dB optical couplers (OC1...OC12), six polarization modulators (PolM-ai, PolM-bj ($i$ = 1, 2, and $j$ = 1, 2, 3, 4)).

Apart from the CW laser and PD, the remaining part of the structure can be regard as a Mach–Zehnder interferometer (MZI) which is constructed with upper and lower branch connected by two 3 dB OCs. The upper branch of MZI consists of subsystem A (marked as "Sub A") and subsystem B (marked as "Sub B") in series. The lower branch of MZI consists of a OATT2 and a OPS2 in series.

Sub A can be regarded as a MZI (marked as "MZI1"), which is constructed with upper and lower arm connected by two 3 dB OCs. The upper arm is made of PolM-a1 and PolM-a2 connected in parallel. The lower arm of MZI1 is made of an OATT1 and an OPS1 in series. Sub B is made of PolM-b1...PolM-b4 connected in parallel.

The optical carrier wave from the CW laser is sent to the PC, and split into two beams by a 3 dB OC, and injected into the upper and lower branches of the MZI, respectively. The input signal in the upper branch is sent to Sub A and Sub B in turn.

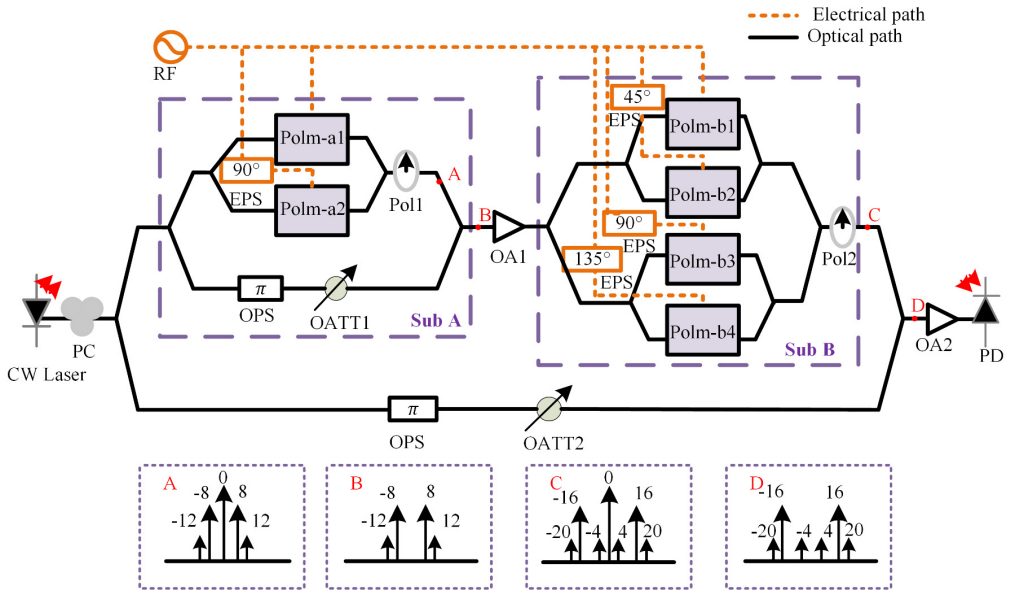


Fig. 1. Schematic diagram of the structure to generate 32-tupling MMW with PolMs. CW laser – continuous wave laser, PC – polarization controller, OPS – optical phase shifter, OATT – optical adjustable attenuator, Pol – polarizer, RF generator – radio frequency signal generator, EPS – electrical phase shifter, OA – optical amplifier, and PD – photodetector.

In the upper branch of MZI, the input signal of Sub A is divided into two branches by a 3 dB OC and sent to the upper and down arms of MZI1 respectively. The input signal of the upper arm is separated into two branches by a 3 dB OC, and sent to the PolM-a1 and PolM-a2, respectively. The input signal passes the down arm past OTTA1 and OPS1 in series. The output signals of two arms of MZI1 are combined with a 3 dB OC. The input signal of Sub B is split by three 3 dB OC and fed into PolM-b1...PolM-b4 connected in parallel. In the down branch of MZI, the input signal is sent to OATT1 and OPS1 in series. The output signals of two branches of MZI are combined with a 3 dB OC, injected into the PD to generate MMW.

Setting the initial phase of the RF driving signals applied on the PolM-a1, PolM-a2, PolM-b1, PolM-b2, PolM-b3 and PolM-b4 as 0, 90°, 0, 45°, 90°and 135°, respectively, and adjusting the amplitudes of the RF drive signal load on PolMs, the 32-tupling frequency MMW is generated in the PD.

## 3. Principle analysis

### 3.1. System output signal

Suppose the optical carrier field from the CW laser is $E_0(t) = E_0 \exp(j\omega_c t)$, where $E_0$ and $\omega_c$ are the optical carrier amplitude and frequency, respectively.

In Sub A, suppose the RF driving signal applied to the PolM-ai ($i = 1, 2$) is $V(t) = V_{RF} \sin[\omega_{RF} t + (i-1)\Delta\varphi]$, where $V_{RF}$ and $\omega_{RF}$ are the amplitude and frequency of the RF signal, respectively; $\Delta\varphi$ is the phase difference of the RF driving signal generated by the EPS applied to the PolM-a1 and PolM-a2.

The $\theta_1$ introduced by PC is set as 45°. Thus, the output of PolM-ai can be expressed as

$$\begin{bmatrix} E_{ix} \\ E_{iy} \end{bmatrix} = \frac{\sqrt{2}}{16} E_0 \exp(j\omega_c t) \begin{bmatrix} \exp\left\{ jm\cos\left[\omega_{RF} t + (i-1)\Delta\varphi\right]\right\} \\ \exp\left\{ -jm\cos\left[\omega_{RF} t + (i-1)\Delta\varphi\right]\right\} \end{bmatrix} \tag{1}$$

where $m = \pi V_{RF}/V_\pi$, and $V_\pi$ are the modulation index and the half-wave voltage of PolM-ai, respectively.

The output signals from PolM-a1 and PolM-a2 are combined with a 3 dB OC, and the output signal of Sub A can be described as

$$E_i(t) = \sum_{i=1}^{2} \begin{bmatrix} E_{ix} \\ E_{iy} \end{bmatrix} = \frac{\sqrt{2}}{16} E_0 \exp(j\omega_c t) \sum_{i=1}^{2} \begin{bmatrix} \exp\left\{ jm\cos\left[\omega_{RF} t + (i-1)\Delta\varphi\right]\right\} \\ \exp\left\{ -jm\cos\left[\omega_{RF} t + (i-1)\Delta\varphi\right]\right\} \end{bmatrix} \tag{2}$$

After the output of sub A passes through Pol1, it can be expressed as

$$\begin{aligned} E_{\mathrm{A}}(t) &= \cos 45^\circ \sum_{i=1}^{2} E_{ix} + \sin 45^\circ \sum_{i=1}^{2} E_{iy} \\ &= \frac{1}{8} E_0 \exp(j\omega_{\mathrm{c}} t) \sum_{i=1}^{2} \cos\left\{ m \cos\left[ \omega_{\mathrm{RF}} t + (i-1)\Delta\varphi \right] \right\} \end{aligned} \tag{3}$$

From Eq. (3), we can see that the output optical signal of Pol1 has been converted from a phase-modulated signal to an intensity-modulated signal. The amplitude modulation factor is $\cos\{m\cos[\omega_{\mathrm{RF}} t + (i-1)\Delta\varphi]\}$.

Using the Jacobi–Anger formula, when $\Delta\varphi = \pi/2$, Eq. (3) can be expanded as follows

$$\begin{aligned} E_{\mathrm{A}}(t) &= \frac{1}{8} E_0 \exp(j\omega_{\mathrm{c}} t) \\ &\quad \times \left\{ 2J_0(m) + \sum_{i=1}^{2} \left[ 2 \sum_{n=1}^{\infty} (-1)^n J_{2n}(m) \cos\left( 2n\omega_{\mathrm{RF}} t + \frac{2n(i-1)\pi}{2} \right) \right] \right\} \\ &= \frac{1}{4} E_0 \exp(j\omega_{\mathrm{c}} t) \Big[ J_0(m) + 2J_4(m)\cos(4\omega_{\mathrm{RF}} t) \\ &\qquad + 2J_8(m)\cos(8\omega_{\mathrm{RF}} t) + 2J_{12}(m)\cos(12\omega_{\mathrm{RF}} t) \ldots \Big] \end{aligned} \tag{4}$$

where $J_{2n}(m)$ is the first kind $2n$-order Bessel function.

From Eq. (4), we can see that the output form Pol1 is $4n$ order optical sidebands. According to the characteristics of $J_n(m)$, when $n > 4$, the $J_{4n}(m)$ is so small to be ignored.

By properly adjusting the modulation index $m_{\mathrm{A}}$ of PolM-ai, the $\pm 4$th-order optical sidebands can be suppressed. By tuning the attenuation of the OATT2 in the lower arm of Sub A, the carrier in the upper and lower arms are equal in amplitude and opposite in phase, and they can be mutual offset in the 3 dB OC. Then the field of the output optical signal from Sub A is expressed as

$$E_{\mathrm{A}}(t) = \frac{1}{2} E_0 \exp(j\omega_{\mathrm{c}} t) \left[ J_8(m_{\mathrm{A}}) \cos(8\omega_{\mathrm{RF}} t) + J_{12}(m_{\mathrm{A}}) \cos(12\omega_{\mathrm{RF}} t) \right] \tag{5}$$

For the Sub B, the optical signal from Sub A is first amplified by the OA1 and then injected to Sub B. Sub B is analysed in the same way as Sub A, except that the phase difference $\Delta\varphi$ of the RF driving signal loaded on each PolM-bi ($i = 1, 2, 3, 4$) is $\pi/4$. The output of Sub B can be denoted as

$$E_{\mathrm{C}}(t) = \frac{1}{4}GE_{\mathrm{B}}(t)\left\{4J_0(m) + \sum_{i=1}^{4}\left[2\sum_{n=1}^{\infty}(-1)^n J_{2n}(m)\cos\left(2n\omega_{\mathrm{RF}}t + \frac{2n(i-1)\pi}{4}\right)\right]\right\}$$

$$= GE_{\mathrm{B}}(t)\left[J_0(m) + 2J_8(m)\cos(8\omega_{\mathrm{RF}}t) + 2J_{16}(m)\cos(16\omega_{\mathrm{RF}}t)...\right] \tag{6}$$

where $G$ is the gain of the OA1.

From Eq. (6), it can be seen that the main component from Sub B is the $\pm 8n$ order optical sideband. By tuning the modulation index $m_{\mathrm{B}}$ of PolM-bi in Sub B, the carrier can be suppressed. Substitution Eq. (5) into Eq. (6), the field of the output optical signal from Sub B can be expressed as

$$E_{\mathrm{C}}(t) = 2E_{\mathrm{B}}(t)\left[J_8(m_{\mathrm{B}})\cos(8\omega_{\mathrm{RF}}t) + J_{16}(m_{\mathrm{B}})\cos(16\omega_{\mathrm{RF}}t)\right]$$

$$= E_0\exp(j\omega_{\mathrm{c}}t)\left[J_8(m_{\mathrm{A}})\cos(8\omega_{\mathrm{RF}}t) + J_{12}(m_{\mathrm{A}})\cos(12\omega_{\mathrm{RF}}t)\right]$$

$$\times\left[J_8(m_{\mathrm{B}})\cos(8\omega_{\mathrm{RF}}t) + J_{16}(m_{\mathrm{B}})\cos(16\omega_{\mathrm{RF}}t)\right]$$

$$= \frac{1}{2}E_0\exp(j\omega_{\mathrm{c}}t)\left\{J_8(m_{\mathrm{A}})J_8(m_{\mathrm{B}})\right.$$

$$+\left[J_8(m_{\mathrm{B}})J_{12}(m_{\mathrm{A}}) + J_{12}(m_{\mathrm{A}})J_{16}(m_{\mathrm{B}})\right]\cos(4\omega_{\mathrm{RF}}t)$$

$$+ J_8(m_{\mathrm{A}})J_{16}(m_{\mathrm{B}})\cos(8\omega_{\mathrm{RF}}t) + J_8(m_{\mathrm{A}})J_8(m_{\mathrm{B}})\cos(16\omega_{\mathrm{RF}}t)$$

$$+ J_8(m_{\mathrm{B}})J_{12}(m_{\mathrm{A}})\cos(20\omega_{\mathrm{RF}}t) + J_8(m_{\mathrm{A}})J_{16}(m_{\mathrm{B}})\cos(24\omega_{\mathrm{RF}}t)$$

$$\left.+ J_{12}(m_{\mathrm{A}})J_{16}(m_{\mathrm{B}})\cos(28\omega_{\mathrm{RF}}t)\right\} \tag{7}$$

By adjusting the attenuation of the OATT2, the carrier in the output optical signal from Sub B can be cancelled by the optical signal from the lower branch of MZI in the 3 dB OC. The output from the 3 dB OC is injected into the PD to realize the photo-electrical conversion. The photocurrent from the PD can be expressed as

$$
\begin{aligned}
I(t) \propto\ & \Re E_0^2 \Big\{ \Big[ J_8(m_\mathrm{B}) J_{12}(m_\mathrm{A}) + J_{12}(m_\mathrm{A}) J_{16}(m_\mathrm{B}) \Big] \cos(4\omega_\mathrm{RF} t) \\
& + J_8(m_\mathrm{A}) J_8(m_\mathrm{B}) \cos(16\omega_\mathrm{RF} t) + J_8(m_\mathrm{B}) J_{12}(m_\mathrm{A}) \cos(20\omega_\mathrm{RF} t) \Big\}^2 \\
=\ & \Re E_0^2 \Big\{ \frac{1}{2} \Big[ J_8^2(m_\mathrm{B}) J_{12}^2(m_\mathrm{A}) + J_{12}^2(m_\mathrm{A}) J_{16}^2(m_\mathrm{B}) + 2 J_8(m_\mathrm{B}) J_{16}(m_\mathrm{B}) J_{12}^2(m_\mathrm{A}) \\
& + J_8^2(m_\mathrm{A}) J_8^2(m_\mathrm{B}) + J_8^2(m_\mathrm{B}) J_{12}^2(m_\mathrm{A}) \Big] \\
& + J_8(m_\mathrm{A}) J_{12}(m_\mathrm{A}) J_8^2(m_\mathrm{B}) \Big[ \cos(4\omega_\mathrm{RF} t) + \cos(36\omega_\mathrm{RF} t) \Big] \\
& + J_8(m_\mathrm{A}) J_{12}(m_\mathrm{A}) J_8(m_\mathrm{B}) \Big[ J_8(m_\mathrm{B}) + J_{16}(m_\mathrm{B}) \Big] \Big[ \cos(12\omega_\mathrm{RF} t) + \cos(20\omega_\mathrm{RF} t) \Big] \\
& + J_{12}^2(m_\mathrm{A}) J_8(m_\mathrm{B}) \Big[ J_8(m_\mathrm{B}) + J_{16}(m_\mathrm{B}) \Big] \Big[ \cos(16\omega_\mathrm{RF} t) + \cos(24\omega_\mathrm{RF} t) \Big] \\
& + \frac{1}{2} \Big[ J_8(m_\mathrm{B}) J_{12}(m_\mathrm{A}) + J_{12}(m_\mathrm{A}) J_{16}(m_\mathrm{B}) \Big]^2 \cos(8\omega_\mathrm{RF} t) \\
& + \frac{1}{2} J_8^2(m_\mathrm{A}) J_8^2(m_\mathrm{B}) \cos(32\omega_\mathrm{RF} t) + \frac{1}{2} J_8^2(m_\mathrm{B}) J_{12}^2(m_\mathrm{A}) \cos(40\omega_\mathrm{RF} t) \Big\} \\
=\ & \Re E_0^2 \Big\{ C_0 + C_4 \Big[ \cos(4\omega_\mathrm{RF} t) + \cos(36\omega_\mathrm{RF} t) \Big] \\
& + C_{12} \Big[ \cos(12\omega_\mathrm{RF} t) + \cos(20\omega_\mathrm{RF} t) \Big] + C_8 \cos(8\omega_\mathrm{RF} t) \\
& + C_{16} \Big[ \cos(16\omega_\mathrm{RF} t) + \cos(24\omega_\mathrm{RF} t) \Big] + C_{32} \cos(32\omega_\mathrm{RF} t) + C_{40} \cos(40\omega_\mathrm{RF} t) \Big\}
\end{aligned}
\tag{8}
$$

where $\Re$ is the responsiveness of the PD.

According to the characteristics of the Bessel function, the amplitude of the 48 times harmonic of RF driving signal is too small to be ignored. From Eq. (8), we can see that the output of the PD contains the harmonic component of frequency 32 times to the RF driving signal, and it is the desired 32-tupling frequency MMW.

### 3.2. Parameter setting and performance index

From Eq. (7), we can see that it is the modulation index of the PolM that controls the magnitude of optical sidebands in the output of the MZI. The attenuation values of OATT1 and OATT2 determine whether the carrier components can be completely can-

celled. Their parameter values have a direct impact on the quality of the generated signal and need to be carefully analysed.

The quality of the generated signals is evaluated by the optical sideband suppression ratio (OSSR) and radio frequency spurious suppression ratio (RFSSR).

#### 3.2.1. Modulation index of PolM

In our scheme, the 32-tupling frequency MMW is generated by beating the ±16th order optical sidebands in the PD. It requires to suppress other sidebands except the ±16th order sidebands. From Eq. (7), we can see that the values of the ±4*n* order sidebands are determined by the value of $J_{4n}(m_A)$. From Fig. 2, we can see that when $m_A = 7.59$, $J_4(7.59) = 0$, the ±4th order optical sidebands are suppressed; when $m_B = 8.65$, $J_0(8.65) = 0$, the carrier is suppressed. When the modulation index takes these values, the value of $J_8(m)$ is much larger than others, which means the amplitude of the ±16th order sideband is much larger than others.

Conclusion: the $m_A$ and $m_B$ are chosen as 7.59 and 8.65, respectively.

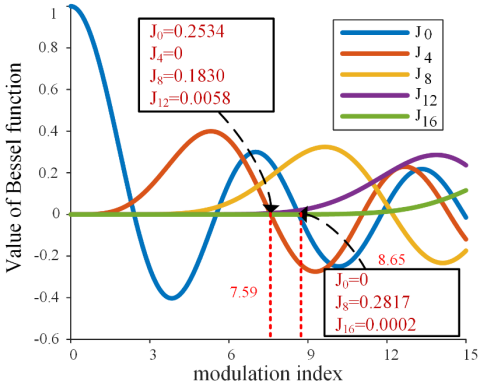


Fig. 2. First kind even-order Bessel function.

#### 3.2.2. The attenuation of the optical attenuator

In our scheme, OATT*i* and OPS*i* (*i* = 1, 2) are used to suppress the optical carrier. According to Eq. (4) and Eq. (7), the amplitude of the carrier in Sub A is $J_0(m_A)E_0/4$, and the amplitude of the carrier sent to OATT2 is $E_0/4$. Therefore, the attenuation value of the OATT1 is

$$\alpha_1 = 20\log_{10}\left[J_0(m_A)\right]^{-1} \tag{9}$$

From Eq. (9), when $m_A$ is chosen to be 7.59 as discussed above, $\alpha_1$ equals 11.92 dB.

In order to cancel the carrier in the output from Sub B, it is need to value the attenuation value of OATT2. According to Eq. (7), in order to generate equal amplitude

and inverse phase carrier to the upper branch of the MZI, the attenuation value of the OATT2 is

$$\alpha_2 = 20\log_{10}\left[J_8(m_A)J_8(m_B)\right]^{-1} - G_{dB} \tag{10}$$

where $G_{dB}$ is the gain of OA1.

From Eq. (10), when $m_A$ is 7.59, $m_B$ is 8.65, and $G_{dB}$ is 20 dB, $\alpha_2$ equals 5.75 dB.

Conclusion: the $\alpha_1$ and $\alpha_2$ are chosen 11.92 and 5.75 dB, respectively.

#### 3.2.3. OSSR and RFSSR

From Eq. (7), the ±16th and ±4th order sidebands are the desired sidebands and the maximum spurious sidebands, respectively. According to the definition of OSSR, we can obtain

$$\text{OSSR} \approx 10\log_{10}\left[\frac{J_8(m_A)J_8(m_B)}{J_8(m_B)J_{12}(m_A)+J_{12}(m_A)J_{16}(m_B)}\right]^2 = 29.89\ \text{dB} \tag{11}$$

According to Eq. (8), $C_4 = 8.4227 \times 10^{-5}$, $C_8 = 2.6882 \times 10^{-6}$, $C_{12} = 2.374 \times 10^{-5}$, $C_{16} = 1.7354 \times 10^{-6}$, $C_{32} = 1.3287 \times 10^{-3}$, $C_{40} = 1.3347 \times 10^{-6}$, when the direct current (DC) component is filtered out , the largest harmonics is the 32 times of RF driving signal, and the second largest harmonic is the 4 times of RF driving signal. According to the definition of RFSSR, we can obtain

$$\text{RFSSR} \approx 10\log_{10}\left[\frac{1}{2}\frac{J_8^2(m_A)J_8^2(m_B)}{J_8(m_B)J_{12}(m_A)J_8^2(m_B)}\right]^2 = 23.88\ \text{dB} \tag{12}$$

## 4. Simulation experiments

According to Fig. 1, a simulation link is built using photonic simulation software. The main parameters in the simulation are set as Table 2.

The basis to select the values of the parameter of the devices in Table 2 is as follows: the basis to choose the frequency of the RF local oscillator as 10 GHz is for the generation of 320 GHz MMW in our simulation. According to the theoretical analysis, the modulation index ($m = \pi V_{RF}/V_\pi$) for "Sub A" and "Sub B" are $m_A = 7.59$ and $m_B = 8.65$, respectively, $V_\pi = 1$ V is the default value in the simulation system, then the values of the amplitudes of the RF local oscillator for "Sub A" and "Sub B" are 2.4154 and 2.7545 V, respectively. The values of the attenuation for attenuator 1 and attenuator 2 are chosen according to Eq. (9) and Eq. (10), respectively. The other values of the parameters in the simulation are chosen according to the default values of the simulation software.

Figures 3 (a)–(d) show the spectrum of the signals at point A, point B, point C, and point D in Fig.1. From Fig. 3 (a), it can be seen that the main components of the

T a b l e 1. Main device parameters involved in simulation.

| Parameter | Value |
|---|---|
| Center frequency of CW laser | 193.1 THz |
| Linewidth of CW laser | 10 MHz |
| Optical power of CW laser | 0 dBm |
| Frequency of RF local | 10 GHz |
| Amplitude of RF local (Sub A) | 2.4154 V |
| Amplitude of RF local (Sub B) | 2.7545 V |
| Gain of optical amplifier | 20 dB |
| Attenuation of attenuator 1 | 11.92 dB |
| Attenuation of attenuator 2 | 5.75 dB |
| Responsivity of photodetector | 0.8 A/W |
| Dark current of photodetector | 10 nA |

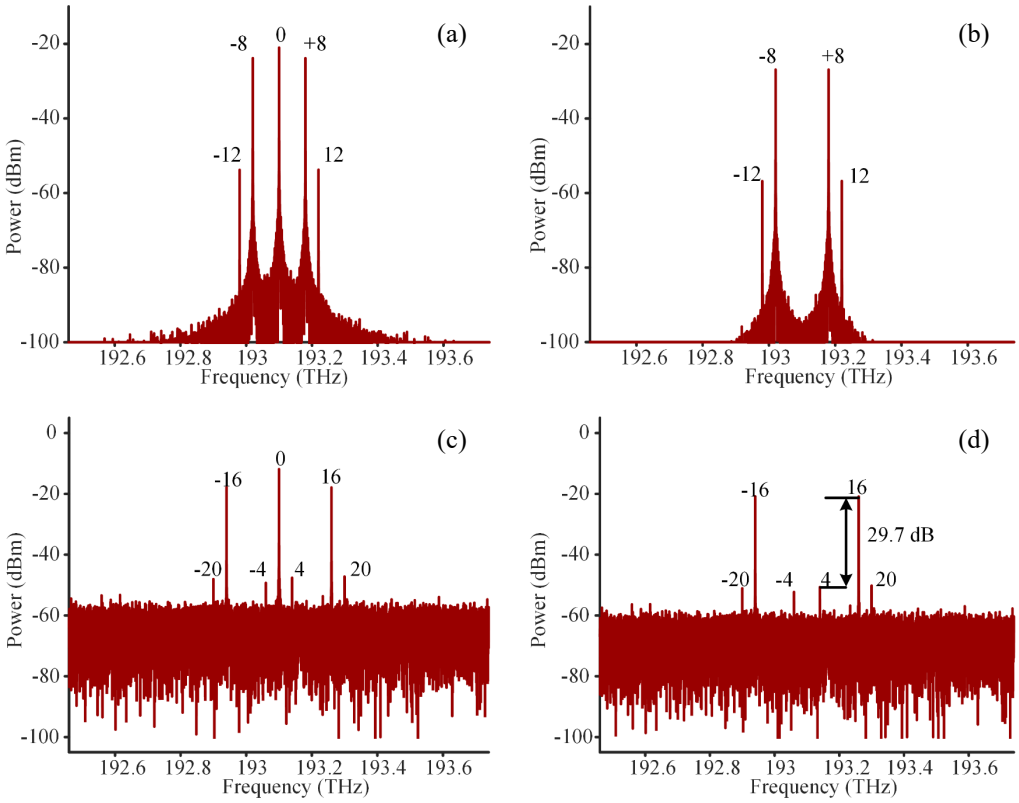


Fig. 3. The spectrum of the output optical signal at (a) point A, (b) point B, (c) point C, and (d) point D.

signal are the 0th, ±8th, and ±12th order optical sidebands. From Fig. 3 (b), it can be seen that the main components are ±8th and ±12th order sidebands. From Fig. 3 (c), it can be seen that the main components are the 0th and ±16th order sidebands. From

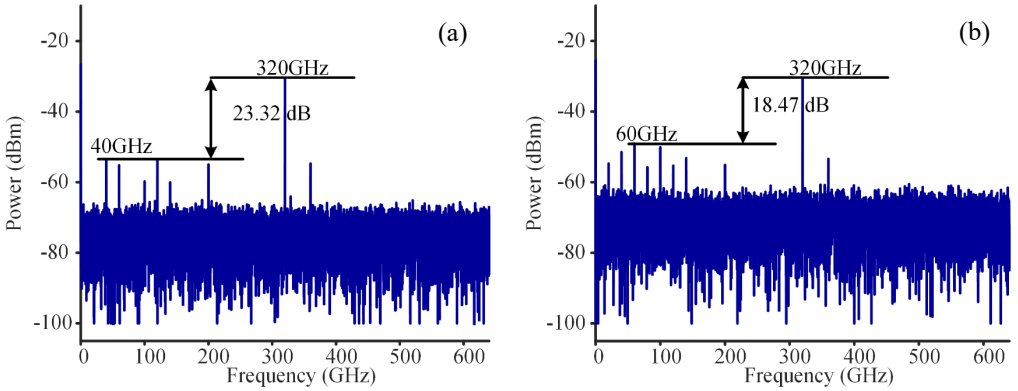


Fig. 4. Spectrum of electrical output signal from PD. (a) OA1 without noise, and (b) OA1 with 4 dB noise.

Fig. 3 (d), it can be seen that the main components are ±4th order, ±16th order and ±20th order sidebands. Among them, the ±16th order sidebands have the largest amplitude and the ±4th order sidebands are the largest spurious sidebands, which are 29.7 dB lower than the ±16th order sidebands. Therefore, the value of OSSR is 29.7 dB, which is consistent with the theoretical calculation value of 29.89 dB in Eq. (11).

Figures 4 (a) and (b) show the output signal spectra of PD when the noise figure of OA1 is 0 and 4 dB, respectively. As seen from Fig. 4 (a), the maximum harmonic in the non-noise case is at 40 GHz (4 times the frequency of RF driving signal), which is 23.32 dB lower than the signal at 320 GHz (32 times the frequency of RF driving signal). Therefore, the value of RFSSR is 23.32 dB, which is consistent with the theoretical calculation value of 23.88 dB in Eq. (12). As seen from Fig. 4, in the 4 dB-noise case, the maximum harmonic is at 60 GHz (6 times the frequency of RF driving signal), and the RFSSR is 18.47 dB.

## 5. ROF for the generated 32-tupling MMW

In order to estimate the transmission performance of the generated 32-tupling frequency MMW over fiber (MMOF), a ROF system is designed with photonic simulation software, which is shown in Fig. 5. In Fig. 5, the 16th order sideband generator is the MZI in Fig. 1.

In the central station (CS) the main devices are the CW laser, 16th order sideband generator, optical interleaver (IL), amplitude modulator (AM), OC, data source, OA, PD, low-pass filter (LPF). In the base station (BS), the main devices are the EDFA, optical circulator, fiber Bragg grating (FBG), PD, RF local oscillator, RF mixer, LPF, OA, AM, and data source.

The frequency of the RF signal is 10 GHz, the data rate for uplink and downlink are both 2.5 Gbps, the fiber length is 30 km, and the reflectivity of the FBG is 5%.

At the CS, the output of the 16th order sideband generator is separated with a IL, and the downlink data signal is modulated to the +16th order sideband with an AM,

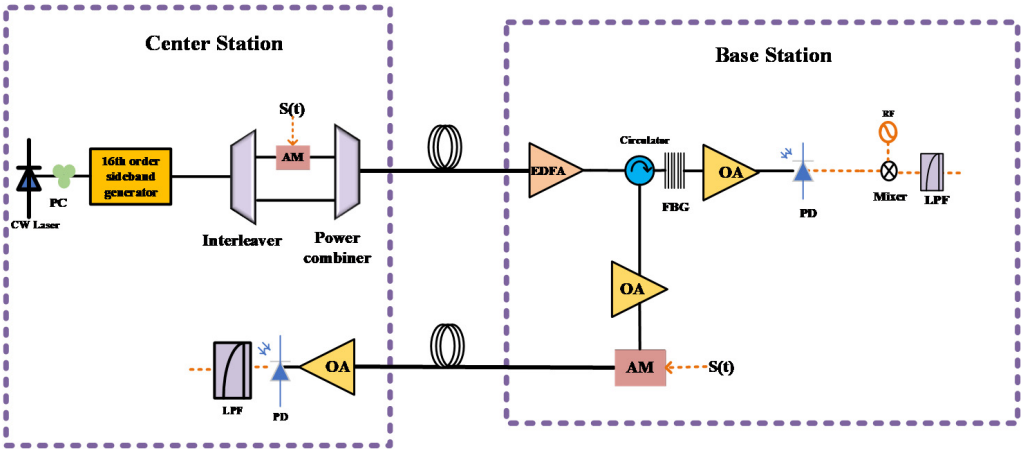


Fig. 5. Full-duplex MMOF system with frequency reuse.

and then the ±16th order sidebands are combined by a power combiner and transmitted to BS via optical fiber. At the same time, the uplink optical signal passes through an OA and is injected into a PD for photoelectric conversion, and then the uplink data signal is filtered through a LPF.

At the BS, a FBG is used to reflect part of the –16th order sideband from the downlink signal. It is used as the carrier for uplink transmission for carrier reuse, and the uplink signal is modulated on it by an AM and transmitted back to the CS via optical fiber for carrier reuse. The output signal from the FBG is injected into the PD, in which the 32-tupling frequency MMW with the downlink data signal is generated. The output

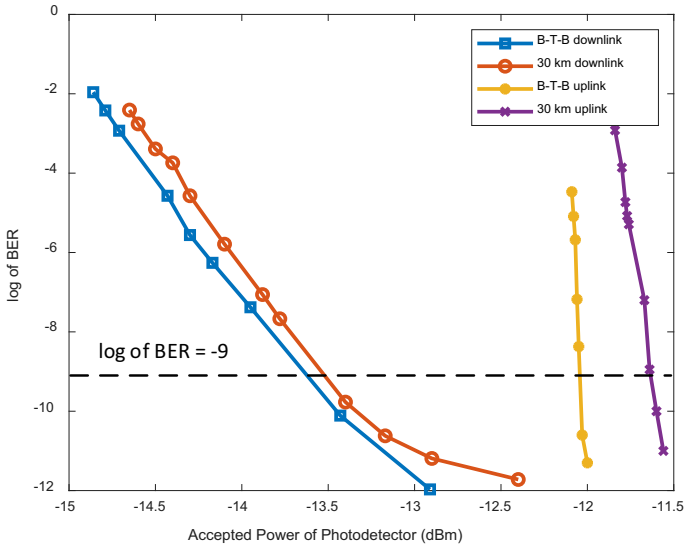


Fig. 6. The relationship between the BER and the received power of PD in the uplink and downlink.

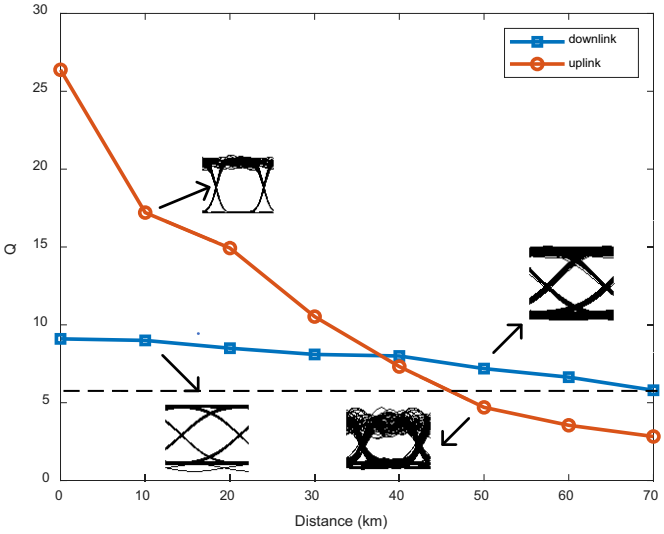


Fig. 7. The relationship of $Q$ value with length of fiber in the uplink and downlink.

signal from the PD is mixed with the 320 GHz local signal from the RF local oscillator in the RF mixer. After the output signal from the mixer passing through the LPF, the downlink data signal is filtered.

Figure 6 shows the relationship of bit error rate (BER) with the received power of PD in the uplink and downlink. We can see from Fig. 6, at BER = $10^{-9}$, for the cases of the back-to-back (BTB) and the 30 km length of fiber, the accepted power of the PD in the uplink are –12 and –11.6 dBm, respectively, with a power penalty of 0.4 dB; the accepted power of the optical detector in the downlink are –13.6 and –13.5 dBm, respectively, with a power penalty of 0.1 dB.

Figure 7 shows the $Q$ value of data *versus* fiber length in the uplink and downlink. When the length of fiber increases from 0 to 70 km, the $Q$ value of the downlink data decreases from 9.1 to 5.8. When the length of fiber increases from 0 to 40 km, the $Q$ value of the uplink data decreases from 26.38 to 7. This indicates that the uplink system performance declines faster and the system stability is poor.

## 6. Discussion

In our designed ROF system, there are some problems to be solved.

1) In our design of ROF system, in order to solve the code walk-off problem for data transmission, a filter is need to filter out the +16th order sideband with which the downlink data is modulated on it. This limit the tenability of frequency to the system. The further research is to find a method to modulate the data on one sideband without filter.

2) In the BS, in order to realize carrier reuse, it is needed to reflect a part of the –16th order sideband. The more power is reflected, the better for the uplink, but it will

reduce the performance of the generated 32-tupling frequency MMW in PD. It is needed to find the optimal reflectivity of FBG for uplink and downlink. Another method is to find a way to realize carrier reuse without filtering the –16th order sideband. An alternative method is that, at CS a OC is used to split the carrier into two parts at the input port and one part is sent into the MZI to generate the ±16th order sidebands, the other OC is used in the output of MZI. At BS, a FBG with 100% reflectivity is used to reflect the carrier for uplink data transmission.

3) In the theoretical analysis and simulation experiment the parameters of the device have ideal values. In practice, owing to the variety of environment and the limitation of manufacturing technology, these parameters often deviate from these ideal values; this will reduce the OSSR and RFSSR of the generated signal. It requires further research.

4) The frequency of the generated MMW is $2nf_{\mathrm{RF}}$ based on PolMs. The $n$ and $f_{\mathrm{RF}}$ are the desired $n$-th order sideband and the RF driving signal frequency. Due to the restrictions of increasing the frequency of RF, the main method to increase the frequency of MMW is to increase $n$. In order to increase the amplitudes of the $n$-th order sideband, it is needed to increase the index modulation of the PolMs. This is a common problem for the methods to generate high frequency MMW based on PolMs. According to the definition of the modulation index of the PolM, $m = \pi V_{\mathrm{RF}}/V_{\pi_{\mathrm{RF}}}$, for a fixed modulation index, the way to reduce $V_{\mathrm{RF}}$ is to reduce the half-wave voltage $V_{\pi_{\mathrm{RF}}}$ of the PolM. From the recent research reports, we can see that a significant progress has been made in reducing the $V_{\pi_{\mathrm{RF}}}$ of PolMs. How to further reduce the modulation index of PolMs will be the issue of our research in the next step.

## 7. Conclusion

In this paper, a novel structure to generate frequency 32-tupling frequency MMW using six PolMs is proposed. The main part of the structure is regarded as a MZI. By adjusting the amplitude and the initial phase of RF driving signal applied to PolMs in the MZI, the attenuation of OATTs, the output of the MZI is ±16th order sidebands. By injecting the ±16th order sidebands into the PD, the 32-tupling frequency MMW is generated. The theoretical calculated OSSR of the generated ±16th order sidebands and RFSSR of the generated 32-tupling frequency MMW are 29.89 and 23.88 dB, respectively. A simulation system based on our scheme is built, and the OSSR and RFSSR from simulation experiments are 29.7 and 23.32 dB, respectively, which are very close to the theoretical calculated values and this verified feasibility of our scheme.

A bidirectional MMOF simulation experiments are carried out, the $Q$ value is greater than 6 and the power penalty is less than 0.4 dB at a transmission distance of 30 km with 2.5 Gbps data for uplink and downlink.

In addition, our scheme has many other advantages, such as high multiplication factor, flexible tuning range and good system stability, good frequency tunability, *etc*. It has wide application prospects in MMW technologies.

**Funding**
National Key Research and Development Project (2018YFB1404101);
National Natural Science Foundation of China (62127802).

## References

[1] QI X.Q., LIU J.M., ZHANG X.P., XIE L., *Fiber dispersion and nonlinearity influences on transmissions of AM and FM data modulation signals in radio-over-fibre system*, IEEE Journal of Quantum Electronics **46**(8), 2010: 1170-1177. https://doi.org/10.1109/JQE.2010.2044747

[2] CUI C.C., CHAN S.C., *Performance analysis on using period one oscillation of optically injected semiconductor lasers for radio-over-fiber uplinks*, IEEE Journal of Quantum Electronics **48**(4), 2012: 490-499. https://doi.org/10.1109/JQE.2012.2185487

[3] LI W., YAO J., *Investigation of photonically assisted microwave frequency multiplication based on external modulation*, IEEE Transactions on Microwave Theory and Techniques **58**(11), 2010: 3259-3268. https://doi.org/10.1109/TMTT.2010.2075671

[4] JÁRÓ G., BERCELI T., *A new high-efficiency optical-microwave mixing approach*, Journal of Lightwave Technology **21**(12), 2003: 3078-3084. https://doi.org/10.1109/JLT.2003.819782

[5] FAN S.H., LIU C., CHANG G.K., *Heterodyne optical carrier suppression for millimeter-wave-over-fiber systems*, Journal of Lightwave Technology **31**(19), 2013: 3210-3216. https://doi.org/10.1109/JLT.2013.2281198

[6] CHEN H.Y., CHI Y.C., LIN C.Y., TSAI C.T., LIN G.R., *Four-wave-mixing suppression of master-to-slave injection-locked two-wavelength FPLD pair for MMW-PON*, Journal of Lightwave Technology **34**(20), 2016: 4810-4818. https://doi.org/10.1109/JLT.2016.2549061

[7] SCHNEIDER T., HANNOVER D., JUNKER M., *Investigation of Brillouin scattering in optical fibers for the generation of millimeter waves*, Journal of Lightwave Technology **24**(1), 2006: 295-304. https://doi.org/10.1109/JLT.2005.859826

[8] BORDONALLI A.C., WALTON C., SEEDS A.J., *High-performance phase locking of wide linewidth semiconductor lasers by combined use of optical injection locking and optical phase-lock loop*, Journal of Lightwave Technology **17**(2), 1999: 328-342. https://doi.org/10.1109/50.744252

[9] ZHIHU W., RONG W., TAO F., *Sextupling tunable mm-wave signal generation based on intensity modulation and Brillouin effect*, Journal of Optoelectronics & Laser **23**(10), 2012: 1890-1894.

[10] LIU W., WANG M., YAO J., *Tunable microwave and sub-terahertz generation based on frequency quadrupling using a single polarization modulator*, Journal of Lightwave Technology **31**(10), 2013: 1636-1644. https://doi.org/10.1109/JLT.2013.2254699

[11] LI W., YAO J., *Microwave and terahertz generation based on photonically assisted microwave frequency twelvetupling with large tunability*, IEEE Photonics Journal **2**(6), 2010: 954-959. https://doi.org/10.1109/JPHOT.2010.2084993

[12] YANG Y., MA J., ZHANG R., XIN X., ZHANG J., *Generation of optical millimeter wave using two cascaded polarization modulators based on frequency octupling without filtering*, Fiber and Integrated Optics **34**(5-6), 2015: 230-242. https://doi.org/10.1080/01468030.2015.1078861

[13] ABOUELEZ A.E., *Photonic generation of millimeter-wave signal through frequency 12-tupling using two cascaded dual-parallel polarization modulators*, Optical and Quantum Electronics **52**, 2020: 166. https://doi.org/10.1007/s11082-020-02285-w

[14] GAYATHRI S., BASKARAN M., *Frequency 16 tupling technique with the use of four parallel polarization modulators*, [In] *2019 International Conference on Wireless Communications Signal Processing and Networking (WiSPNET)*, IEEE, 2019: 282-286. https://doi.org/10.1109/WiSPNET45539.2019.9032798

[15] BASKARAN M., PRABAKARAN R., GAYATHRI T.S., *Photonic generation of frequency 16-tupling millimeter wave signal using polarization property without an optical filter*, Optik **184**, 2019: 348-355. https://doi.org/10.1016/j.ijleo.2019.04.077

[16] Chaudhuri R.B., Barman A.D., Bogoni A., *Photonic 60 GHz sub-bands generation with 24-tupled frequency multiplication using cascaded dual parallel polarization modulators*, Optical Fiber Technology **58**, 2020: 102244. https://doi.org/10.1016/j.yofte.2020.102244

[17] Chen X., Liu X., Li Z., *A flterless frequency 32-tupling photonic scheme to generate sub-terahertz wave signal enabled by optical polarization modulators*, Optical and Quantum Electronics **53**, 2021: 663. https://doi.org/10.1007/s11082-021-03321-z

[18] Chen X., Liu X., Dai S., Li Z., Ba W., Wang D., *Generation of frequency 32-tupling millimetre-wave based on a dual-parallel polarization modulator*, Applied Optics **61**(1), 2022: 294-301. https://doi.org/10.1364/AO.446345

*Received June 28, 2023*
*in revised form August 29, 2023*